University of Wollongong
Research Online

Australian Institute for Innovative Materials - Papers

Australian Institute for Innovative Materials

2018

Readily Exfoliated TiSe2 Nanosheets for High-Performance Sodium Storage

Dan Zhang
University of Wollongong, dz966@uowmail.edu.au

Guoqiang Zhao
University of Wollongong, gz815@uowmail.edu.au

Peng Li
University of Wollongong, pl465@uowmail.edu.au

Yu Zhang
University of Wollongong, azhang@uow.edu.au

Wenbin Qiu
University of Wollongong, wq118@uowmail.edu.au

See next page for additional authors

Readily Exfoliated TiSe2 Nanosheets for High-Performance Sodium Storage

Abstract

Materials with sheet-like morphologies are highly desirable candidates for energy storage and conversion applications, due to the confined atomic thickness and high surface area, which would largely improve the electrochemical reaction kinetics. In this work, the sodium storage performance of TiSe 2 nanosheets and corresponding sodiation/desodiation reaction mechanism are studied for the first time. TiSe 2 nanosheets are readily exfoliated from bulk TiSe 2 after quick ultrasonication or grinding. The TiSe 2 nanosheets exhibit a reversible capacity of 147mAhg -1 at 0.1Ag -1 , and show excellent rate capability with a capacity of 103mAhg -1 at an ultra-high current density of 10.0Ag -1 . The combined in situ XRD and ex-situ HRTEM results suggest that sodium storage in TiSe 2 is achieved through a multi-step intercalation/deintercalation mechanism. Besides, TiSe 2 might be a promising 2D nanomaterial platform for other energy and electronic applications due to its easy exfoliation and unique physicochemical properties.

Disciplines
Engineering | Physical Sciences and Mathematics

Authors

Dan Zhang, Guoqiang Zhao, Peng Li, Yu Zhang, Wenbin Qiu, Jie Shu, Yinzhu Jiang, Shi Xue Dou, and Wenping Sun

Readily Exfoliated TiSe₂ Nanosheets for High-Performance Sodium Storage

Dan Zhang,[a,b,d+] Guoqiang Zhao,[b,+] Peng Li,[b] Yu Zhang,[b] Wenbin Qiu,[b] Jie Shu,[c] Yinzhu Jiang,[a,*] Shi Xue Dou[b], Wenping Sun[b,*]

Abstract: Materials with sheet-like morphologies are highly desirable candidates for energy storage and conversion applications due to the confined atomic thickness and high surface area, which would largely improve the electrochemical reaction kinetics. In this work, the sodium storage performance of $TiSe_2$ nanosheets and corresponding sodiation/desodiation reaction mechanism are studied for the first time. $TiSe_2$ nanosheets are readily exfoliated from bulk $TiSe_2$ after quick ultrasonication or grinding. The $TiSe_2$ nanosheets exhibit a reversible capacity of 147 mAh g⁻¹ at 0.1 A g⁻¹, and show excellent rate capability with a capacity of 103 mAh g⁻¹ at an ultra-high current density of 10.0 A g⁻¹. The combined *in-situ* XRD and *ex-situ* HRTEM results suggest that sodium storage in $TiSe_2$ is achieved through a multi-step intercalation/deintercalation mechanism. Besides, $TiSe_2$ might be a promising 2D nanomaterial platform for other energy and electronic applications due to its easy exfoliation and unique physicochemical properties.

Introduction

Sodium ion batteries (SIBs) recently have received considerable attention as one of the most promising alternatives to lithium ion batteries (LIBs) for energy storage due to the abundance of sodium resources.[1-3] However, due to the larger ionic radius of Na^+ as compared with Li^+, the sodiation/desodiation reaction shows very sluggish kintics, and it is a great challenge to develop practical electrodes showing high capacity, fast and durable sodium storage behavior. Currently, exploring high-performance electrodes is becoming the most critical issue for the further development of SIBs.[4-7]

Recently, Two-dimensional (2D) nanomaterials and other materials with sheet-like morphologies are emerging fast into energy and electronic fields owing to the unique physicochemical properties compared with their bulk counterparts, mainly including confined atomic thickness, high specific surface area and quantum confinement of electrons in 2D plane.[8-9] Graphene, the most typical 2D nanomaterial, has been successfully applied in energy storage and conversion technologies, especially lithium-ion batteries (LIBs), sodium-ion batteries (SIBs),[10-11] and supercapacitors (SCs).[12-15] Many transition metal dichalcogenides (TMDs) also have layered structure and they have been widely explored as electrode materials for SIBs because the presence of d-orbital electrons of transition metals and their layered structure facilitate the intercalation of alkali metal cations.[16-19] In order to fulfil the full potential for sodium storage, lots of efforts have been put into synthesizing TMD nanosheets and the related composites. As one of the most studied TMDs, MoS_2 has been widely studied as the anode for SIBs, delivering very attractive electrochemical performance.[20-22] $MoSe_2$, an analogue to MoS_2, is expected to have higher coulombic efficiency and electronic conductivity because of its larger interlayer space and smaller band gap.[23-24] Xie *et al.* reported the enhanced performance of C-$MoSe_2$-rGO for sodium storage, and a high specific capacity of 445 mAh g⁻¹ at 200 mA g⁻¹ after 350 cycles was achieved, with an initial coulombic efficiency of ~62.4%.[25] TiS_2 is another popular electrode material among TMDs and was extensively investigated as LIBs electrode.[26-27] Liu *et al.* recently reported thin TiS_2 nanoplates as SIBs cathode, delivering satisfying sodium storage performance (~100 mAh g⁻¹ at 10 C) based on the reversible intercalation/deintercalation of Na^+.[28] $TiSe_2$, with a larger interlayer spacing (0.601 nm) over TiS_2 (0.569 nm) and better electronic conductivity,[29] is expected to be superior to TiS_2 for fast intercalation/deintercalation of alkali metal cations. Gu *et al.* reported that the *d-p* orbital hybridization in $TiSe_2$ is a possible key factor to realize reversible intercalation of Mg^{2+} into $TiSe_2$.[30] As inspired by all these previous reports, $TiSe_2$ nanosheets are expected to be promising electrode materials for SIBs. To our best knowledge, the sodium storage capability and sodiation/desodiation mechanism of $TiSe_2$ has not been reported yet. Herein, $TiSe_2$ bulk powders were synthesised by solid state reaction and were found to be extremely easily exfoliated into nanosheets by ultrasonication or grinding within a very short period of time. The sodiation/desodiation reaction mechanism of $TiSe_2$ was studied for the first time and a multi-step process was observed. The $TiSe_2$ nanosheets electrode delivers a reversible capacity of 147 mAh g⁻¹ at a current density of 0.1 A g⁻¹, and shows very attractive rate capability (110 and 103 mAh g⁻¹ at 5.0 and 10.0 A g⁻¹, respectively) as well as cycling performance (115 mAh g⁻¹ during the 500th cycle at 0.5 A g⁻¹).

[a] Dr. D. Zhang⁺, Prof. Y. Jiang
State Key Laboratory of Silicon Materials, Key Laboratory of Novel Materials for Information Technology of Zhejiang Province, Key Laboratory of Advanced Materials and Applications for Batteries of Zhejiang Province, School of Materials Science and Engineering, Zhejiang University, Hangzhou, Zhejiang, P. R. China
E-mail: yzjiang@zju.edu.cn

[b] Dr. D. Zhang⁺, G. Zhao⁺, P. Li, Dr. Y. Zhang, W. Qiu, Prof. S. Dou, Dr. W. Sun
Institute for Superconducting and Electronic Materials, Australian Institute of Innovative Materials, University of Wollongong, Wollongong, NSW 2522, Australia
E-mail: wenping@uow.edu.au

[c] Prof. J. Shu
Faculty of Materials Science and Chemical Engineering, Ningbo University, Ningbo 315211, Zhejiang, P. R. China

[d] Dr. D. Zhang
Guotai Junan Securities Co. Ltd., Shanghai, 200120, P. R. China
+These authors contribute equally to this work.
Supporting information for this article is given via a link at the end of the document.

Results and Discussion

The XRD pattern of the as-prepared powders is presented in **Figure 1**a. All the diffraction peaks can be assigned to $TiSe_2$ with hexagonal structure (JCPDS No. 30-1383), and no impurity phases can be found. XPS analysis was performed to further confirm the chemical composition of $TiSe_2$ powders (Figure S1, Supporting Information). In the Ti XPS spectrum, the peak at 456.5 and 463.5 eV is ascribed to Ti $2P_{3/2}$ and $2P_{1/2}$ of Ti^{4+}, respectively.[31] The peak at 54.0 eV in the Se spectrum can be assigned to Se 3d of Se^{2-} while the peak at 58.5eV corresponds to Se $3d_{5/2}$ of Se^{4+} that might originate from the surface oxidation of the sample.[32-33] As shown in Figure S2a (Supporting Information), the plate-like $TiSe_2$ particles (around 200 nm in thickness and 1 μm in lateral size) loosely agglomerate together in the as-prepared powders. $TiSe_2$ powders are exfoliated into nanosheets after ultrasonication in EtOH for 5 min during preparing TEM samples (Figure 1b, Figure S2b). The detailed characterization of $TiSe_2$ nanosheets was conducted by scanning transmission electron microscope (STEM) as shown in Figure 1c and 1d. The nanosheet is about 17 nm in thickness and contains ca. 28 $TiSe_2$ layers. And the lattice spacing is determined to be 0.61 nm, corresponding to the (001) crystal planes. The high-resolution high angle annular dark field-STEM (HAADF-STEM) image presented in Figure 1d is consistent with the crystal mode viewed along the [100] axis (inset in Figure 1d), which clearly reflects the typical Se-Ti-Se sandwich structure at the atomic level.
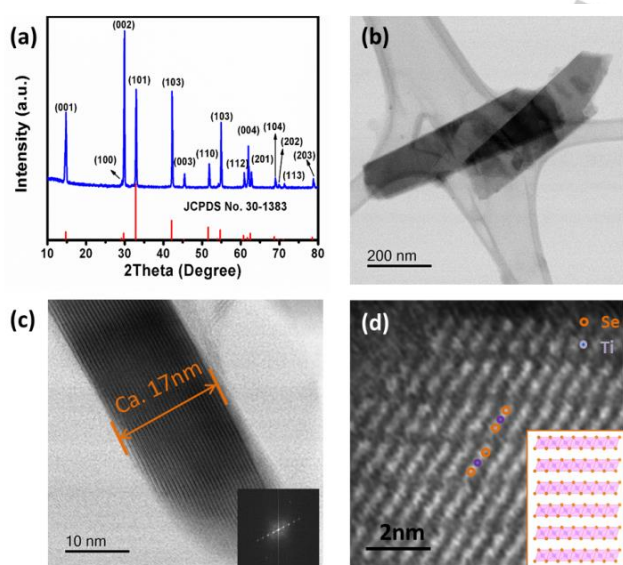
The exfoliation and dispersion of $TiSe_2$ nanosheets were further evaluated in several other solvents, including DMF, methanol, NMP, and acetone etc. It is found that the bulk $TiSe_2$ powders can also be easily exfoliated in NMP and DMF after ultrasonication in a very short period of time, as evidenced by the digital picture of the $TiSe_2$ suspensions in various solvents (Figure S3a, Supporting Information). Moreover, the $TiSe_2$ suspensions with EtOH, NMP and DMF solvents still keep stable overnight (Figure S3b, Supporting Information). The TEM images of the exfoliated nanosheets (**Figure 2**a-c) confirm the successfully exfoliation of the $TiSe_2$. The results suggest that liquid exfoliation in particular with EtOH solvent is an effective way to prepare $TiSe_2$ nanosheets in large scale, and $TiSe_2$ might work as a very promising 2D nanomaterial platform for energy and electronic applications. The reason for the easy exfoliation of $TiSe_2$ may derive from the relatively weaker van der Waals forces between interlayers. T. Bjorkman et al. calculated the interlayer binding and exfoliation energies for a large number of layered compounds, and the results proved that the interlayer binding energy of $TiSe_2$ was smaller than those of most TMD materials.[34] Meanwhile, the bulk $TiSe_2$ powders can be readily delaminated into nanosheets only by grinding using mortar and pestle for 5 min, as shown in Figure 2d. In this work, $TiSe_2$ powders are ground firstly and then mixed homogenously with carbon nanotubes and PVDF in NMP to prepare $TiSe_2$ electrode slurry. This unique nanostructure would play a vital role in achieving shortened ion diffusion pathways, abundant electrode/electrolyte contact and sufficient electrochemically active sites, thereby resulting in enhanced sodiation/desodiation reaction kinetics.
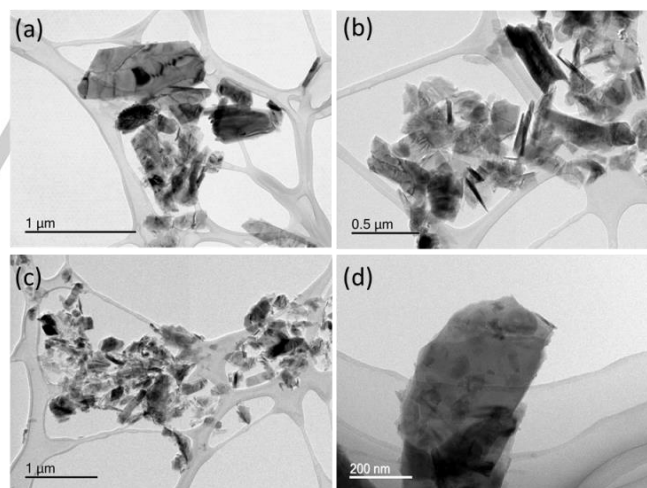

Figure 1. (a) XRD pattern of $TiSe_2$ bulk powders, (b) TEM image of $TiSe_2$ nanosheets, (c) STEM image of one single $TiSe_2$ nanosheet along [100] zone axis and the corresponding FFT image (d) HAADF-STEM image of $TiSe_2$ nanosheet and the corresponding crystal mode.

Figure 2. TEM images of $TiSe_2$ nanosheets exfoliated in different solvents: (a) DMF, (b) NMP and (c) Acetone; (d) TEM image of $TiSe_2$ nanosheets after grinding bulk $TiSe_2$ using mortar and pestle for 5 min.

Generally, it takes several hours or even longer time to prepare TMDs nanosheets by the typical liquid exfoliation process. In our case, bulk $TiSe_2$ powders can be exfoliated into nanosheets after unltrasonication in EtOH for just 5 min as discussed above.

As a proof-of-concept demonstration, the sodium storage performance of $TiSe_2$ nanosheets was evaluated with sodium foil as counter electrode. To unravel the sodiation/desodiation mechanism of $TiSe_2$, *in-situ* XRD upon the initial two cycles was conducted as shown in **Figure 3**a, and the peaks' shift is shown clearly in the overall in-situ XRD image (Figure S4, Supporting Information). A three-stage discharge process is observed

accompanied with sodium intercalation. A new phase $Na_{0.32}TiSe_2$ (JCPDS No. 32-1181) with similar hexagonal structure is firstly formed when the voltage reaches 1.7 V. Then, as the cell is discharged to 1.5 V, a second new phase indexed to $Na_{0.72}TiSe_2$ (JCPDS No. 32-1182) is obtained, the structure of which is also hexagonal with larger interlayer space.[35] When the cell is discharged to 1.0V, $NaTiSe_2$ is eventually formed.
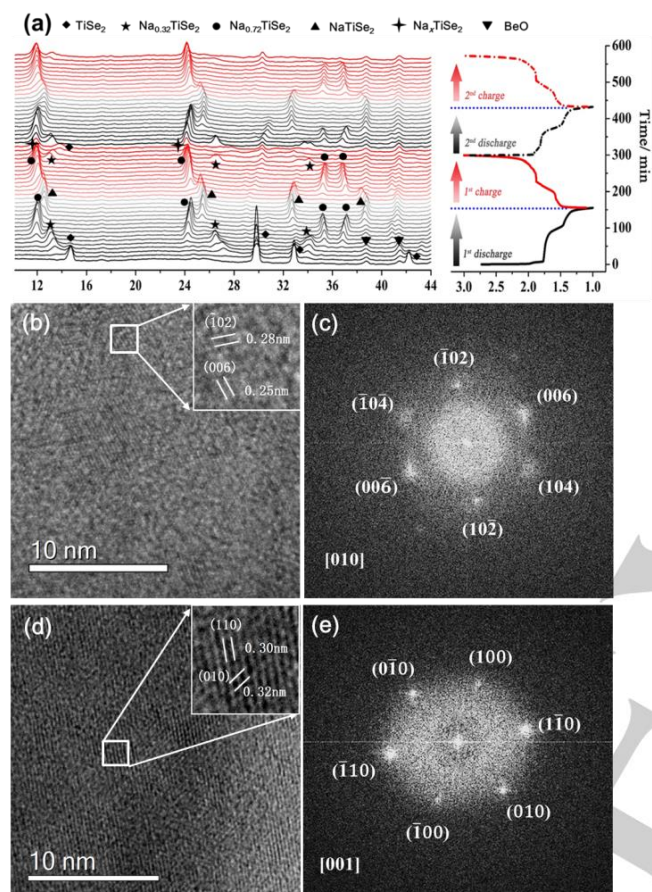

Figure 3. (a) *In-situ* XRD pattern of $TiSe_2$ electrode during initial two cycles, (b) HRTEM image of $NaTiSe_2$ at the end of the first discharge and (c) the corresponding FFT pattern, (d) HRTEM image of $TiSe_2$ with enlarged interlayer space at the end of the first charge and (e) the corresponding FFT pattern.

The formation of hexagonal $NaTiSe_2$ with P63mmc space group is also confirmed by the *ex-situ* HRTEM result and corresponding fast Fourier transform (FFT) pattern, as shown in Figure 3b. The lattice spacing of 0.28 and 0.25 nm can be assigned to the $(\bar{1}02)$ and (006) planes of $NaTiSe_2$. In the following charge process, $NaTiSe_2$ is transformed to $Na_{0.72}TiSe_2$ firstly and then $Na_{0.32}TiSe_2$ as the charge process goes on. At the end of the charge process, $TiSe_2$ with (001) orientation and larger interlayer space is formed due to the exfoliation of $TiSe_2$ during the sodiation/desodiation process. The intercalation of alkaline ions is a widely deployed approach for exfoliation of 2D TMDs nanosheets.[36-37] As can be seen from both the HRTEM and FFT results (Figure 3d), the interlayer spacing of (100) increases to be 0.32 nm. Furthermore, the FFT shows a spot pattern along the [001] zone axis, indicating the exposure of

(001) facets. These phenomena are in perfect consistence with the *in-situ* XRD results, where only the (001) diffraction peak of $TiSe_2$ are preserved and shifts to low angle after full charging. Besides the characteristic peak of $TiSe_2$, there are two unidentified peaks located at 11.9° and 24.1°, and this unknown phase might have a nominal composition of Na_xTiSe_2 (x<0.1) as estimated based on the reversible charge capacity, which needs to be further investigated in the future work. Overall, the sodium insertion/extraction in $TiSe_2$ may go through the following processes:

First discharge: $TiSe_2 \rightarrow Na_{0.32}TiSe_2 \rightarrow Na_{0.72}TiSe_2 \rightarrow NaTiSe_2$.
Reversible charge/discharge: $NaTiSe_2 \leftrightarrow Na_{0.72}TiSe_2 \leftrightarrow Na_{0.32}TiSe_2 \leftrightarrow TiSe_2+Na_xTiSe_2$.
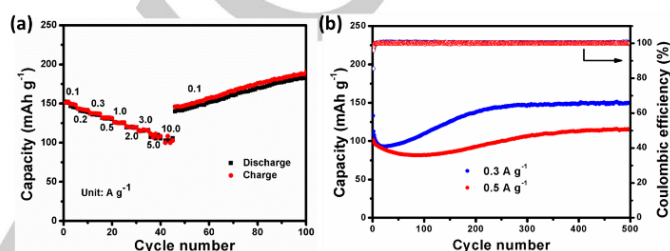

Figure 4. Electrochemical performances of $TiSe_2$ nanosheets electrodes. (a) rate capability of $TiSe_2$ nanosheets electrode, (b) the cycling performance of $TiSe_2$ nanosheets electrode at different current densities of 0.3 and 0.5 A g^{-1}.

The $TiSe_2$ nanosheets exhibit extraordinary rate performance as shown in **Figure 4**a. As the current density is gradually increased from 0.1 to 0.2, 0.3, 0.5, 1.0, 2.0 and 3.0 A g^{-1}, the reversible capacity sightly changes from 150 to 140, 136, 131, 125, 120 and 115 mAh g^{-1}. Even at higher current densities of 5.0 and 10.0 A g^{-1}, the reversible capacity still remains to be 110 and 103 mAh g^{-1}, respectively. When the current density is set back to 0.1 A g^{-1}, the capacity recovers to 140 mAh g^{-1} and keeps rising to 185 mAh g^{-1} during the following 100 cycles. The cycling performance is further evaluated at 0.3 and 0.5 A g^{-1}. As shown in Figure 4b, the cell shows a quite exciting cycling performance and the capacity retains to be 150 and 115 mAh g^{-1} after 500 cycles at 0.3 and 0.5 A g^{-1}, respectively. The first-cycle coulombic efficiency is 86% and 92% at 0.3 and 0.5 A g^{-1}, respectively, and rises to almost 100% upon cycling. Notably, the discharge plateau still keeps at around 1.7 and 1.4 V even at 0.5 A g^{-1} (Figure S5, supporting information). The *ex-situ* TEM image shows that the nanosheets morphology is well maintained after cycling at 0.3 A g^{-1} (Figure S6, Supporting Information). It is worth of noting that the capacity also starts rising after around 100 cycles, and this behaviour appears to be more significant at low current density. Based on the aforementioned discussion, $TiSe_2$ nanosheets would be exfoliated into thinner nanosheets after continuously intercalation/deintercalation of sodium ions, creating more adsorption sites for sodium ions and shortening ion diffusion pathway as well, and this is one possible reason for capacity rising. Under this circumstance, the intercalation/deintercalation processes at low current densities is more gentle and thorough; therefore, the capacity rising phenomenon is more obvious at lower current densities. Similar phenomenon was observed in previous study of MoS_2 electrode,[20] where the MoS_2 layers were gradually expanded

and exfoliated upon cycling, resulting in smaller polarization and faster reaction kinetics for Na$^+$ storage. And more efforts need to be made to further investigate this abnormal behaviour.

CV curves at various scan rates from 0.1 to 2.0 mV s^{-1} are conducted to gain further insight into the electrochemical kinetics of TiSe$_2$ nanosheets for sodium storage as shown in **Figure 5**a. Clearly, the CV curves at different scan rates display similar shape, and both cathodic and anodic current increase accordingly with scan rate. It is very interesting to note that the peak shifting is negligible upon increasing scan rates, demonstrating small polarization at high rate. According to previous studies,[38-40] the measured currents (i) and the scan rates (v) have the following relationship:
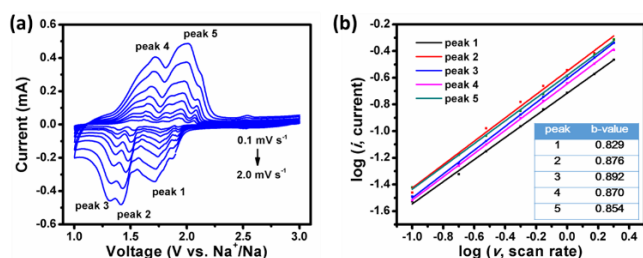
$$i = a\,v^b$$

Figure 5. (a) CV curves at different scan rates from 0.1 to 2.0 mV s^{-1}, (b) fitted linear lines for $\log(v)$-$\log(i)$ plots.

The b-value can be calculated by fitting the $\log(v)$-$\log(i)$ plots. Basically, b value of 1.0 represents the electrochemical system is dominated by capacitive process, whereas 0.5 indicates ionic diffusion controls the whole process. The $\log(v)$-$\log(i)$ plots for the TiSe$_2$ nanosheets electrode are shown in Figure 5b. The b values for all five cathodic and anodic peaks are estimated to be over 0.8, suggesting the electrochemical kinetics is mainly controlled by the capacitive process, which leads to fast Na$^+$ intercalation/extraction kinetics and hence excellent rate performance.

Conclusions

In summary, layered TiSe$_2$ was, for the first time, evaluated as a robust electrode for SIBs. Multi-step insertion/extraction process of Na$^+$ in TiSe$_2$ is observed based on *in-situ* XRD and ex-situ HRTEM analysis. The TiSe$_2$ electrode delivers promising specific capacity (147mAh g^{-1} at 0.1 A g^{-1}), good rate capability (110 and 103 mAh g^{-1} at 5 and 10 A g^{-1}), and excellent cycling performance (115 mAh g^{-1} after 500 cycles at 0.5 A g^{-1}). Besides, TiSe$_2$ can be easily delaminated into nanosheets after quick ultrasonication or grinding. In addition to be a promising electrode for SIBs, TiSe$_2$ might work as a potential 2D material platform for other energy and electronic applications.

Experimental Section

Materials synthesis: TiSe$_2$ powders were prepared by solid state reaction method. The stoichiometric amounts of Ti (99.98% Alfa) and Se (99.98% Alfa) powders were thoroughly mixed and sealed in an evacuated quartz tube, which was then sintered at 570 ^{o}C for 48 h in a muffle furnace. TiSe$_2$ nanosheets were acquired after grinding using mortar and pestle or ultrasonication in various solvents including ethanol (EtOH), dimethylformamide (DMF), N-Methyl-2-pyrrolidone (NMP), and acetone for 5~15 minutes.

Materials characterization: The X-ray diffraction (XRD) patterns of the TiSe$_2$ powders were recorded using a GBC enhanced mini-materials analyser X-Ray diffractometer with a Cu Kα radiation (λ=1.541Å, 25mA, 40kV, 2°/min from 10° to 80°). The surface chemical state was detected by X-ray photoelectron spectroscopy (XPS, Phoibos 100 Analyser, SPECS, Germany, Al K$_\alpha$ X-rays), and the obtained results were fitted with the Casa XPS software. The morphology of the samples was observed by a JEOL JSM-7500FA field-emission scanning electron microscope (FESEM) and a JEOL 2010 transmission electron microscope (TEM). Scanning TEM (STEM) images were acquired on a probe-corrected JEOL ARM200F operated at 200 kV equipped with a cold field emission gun and a high resolution pole-piece. A special battery with beryllium window was used for *in-situ* XRD tests, which were collected at a Bruker AXS D8 Focus power X-ray Diffractometer with a Cu K$_\alpha$ radiation (λ=1.541Å). The samples were scanned from 10 to 60° with a step size of 0.1° and a count time of 1s.

Electrochemical measurements: As a proof-of-concept demonstration, the sodium storage performances of TiSe$_2$ were evaluated. The TiSe$_2$ powders were thoroughly mixed with carbon nanotubes (CNTs) and polyvinyl-difluoride (PVDF) in a weight ratio of 7:2:1 in NMP, which were ground by mortar and pestle to form homogeneous slurry. The cell working electrodes were prepared by painting the slurry on copper foil, followed by vacuum drying at 80 °C overnight. The standard CR2032 coin-type cells were assembled in an Ar-filled glove box with both H$_2$O and O$_2$ levels less than 1 ppm. Metallic Na foil was employed as the counter/reference electrode, and Whatman GF/D microfiber filter paper was used as the separator. 1 M NaClO$_4$ dissolved in tetraethylene glycol dimethyl ether (TEGDME) was used as the electrolyte. Galvanostatic charge/discharge testing was conducted in the voltage range of 1.0-3.0 V (vs. Na/Na$^+$) at room temperature using a NEWARE multichannel battery test system.

Acknowledgements

1.   M. D. Slater, D. Kim, E. Lee and C. S. Johnson, *Adv. Funct. Mater.*, 2013, **23**, 947.
2.   B. Dunn, H. Kamath and J.-M. Tarascon, *Science*, 2011, **334**, 928.
3.   H. Pan, Y.-S. Hu and L. Chen, *Energy Environ. Sci.*, 2013, **6**, 2338.
4.   S. W. Kim, D. H. Seo, X. Ma, G. Ceder and K. Kang, *Adv. Energy Mater.*, 2012, **2**, 710.
5.   X. Xiang, K. Zhang and J. Chen, *Adv. Mater.*, 2015, **27**, 5343.
6.   Y. Kim, K. H. Ha, S. M. Oh and K. T. Lee, *Chem. - Eur. J.*, 2014, **20**, 11980.
7.   L. P. Wang, L. Yu, X. Wang, M. Srinivasan and Z. J. Xu, *J. Mater. Chem. A*, 2015, **3**, 9353.
8.   M. Chhowalla, H. S. Shin, G. Eda, L.-J. Li, K. P. Loh and H. Zhang, *Nat. Chem.*, 2013, **5**, 263.
9.   Q. H. Wang, K. Kalantar-Zadeh, A. Kis, J. N. Coleman and M. S. Strano, *Nat. Nanotechnol.*, 2012, **7**, 699.
10.   J. Xu, M. Wang, N. P. Wickramaratne, M. Jaroniec, S. Dou and L. Dai, *Adv. Mater.*, 2015, **27**, 2042.
11.   Y. Yan, Y. X. Yin, Y. G. Guo and L. J. Wan, *Adv. Energy Mater.*, 2014, **4**.
12.   D. Chen, L. Tang and J. Li, *Chem. Soc. Rev.*, 2010, **39**, 3157.
13.   M. Pumera, *Energy Environ. Sci.*, 2011, **4**, 668.
14.   E. Morales-Narváez, L. F. Sgobbi, S. A. S. Machado and A. Merkoçi, *Prog. Mater. Sci.*, 2017.
15.   V. Singh, D. Joung, L. Zhai, S. Das, S. I. Khondaker and S. Seal, *Prog. Mater. Sci.*, 2011, **56**, 1178.
16.   M. Pumera, Z. Sofer and A. Ambrosi, *J. Mater. Chem. A*, 2014, **2**, 8981.
17.   M. Aydinol, A. Kohan, G. Ceder, K. Cho and J. Joannopoulos, *Phys. Rev. B*, 1997, **56**, 1354.
18.   A. Samad, A. Shafique and Y.-H. Shin, *Nanotechnology*, 2017, **28**, 175401.
19.   K. Chen, W. Zhang, L. Xue, W. Chen, X. Xiang, M. Wan and Y. Huang, *ACS applied materials & interfaces*, 2017, **9**, 1536.
20.   Z. Hu, L. Wang, K. Zhang, J. Wang, F. Cheng, Z. Tao and J. Chen, *Angew. Chem.*, 2014, **126**, 13008.

21.   G. Zhang, H. Liu, J. Qu and J. Li, *Energy Environ. Sci.*, 2016, **9**, 1190.
22.   L. Huang, Q. Wei, X. Xu, C. Shi, X. Liu, L. Zhou and L. Mai, *Phys. Chem. Chem. Phys.*, 2017.
23.   Y. Shi, C. Hua, B. Li, X. Fang, C. Yao, Y. Zhang, Y. S. Hu, Z. Wang, L. Chen and D. Zhao, *Adv. Funct. Mater.*, 2013, **23**, 1832.
24.   H. Wang, X. Lan, D. Jiang, Y. Zhang, H. Zhong, Z. Zhang and Y. Jiang, *J. Power Sources*, 2015, **283**, 187.
25.   D. Xie, W. Tang, Y. Wang, X. Xia, Y. Zhong, D. Zhou, D. Wang, X. Wang and J. Tu, *Nano Res.*, 2016, **9**, 1618.
26.   J. E. Trevey, C. R. Stoldt and S.-H. Lee, *J. Electrochem. Soc.*, 2011, **158**, A1282.
27.   J. Chen, Z. L. Tao and S. L. Li, *Angew. Chem.*, 2003, **115**, 2197.
28.   Y. Liu, H. Wang, L. Cheng, N. Han, F. Zhao, P. Li, C. Jin and Y. Li, *Nano Energy*, 2016, **20**, 168.
29.   X. Yuan, M. Yang, L. Wang and Y. Li, *Phys. Chem. Chem. Phys.*, 2017, **19**, 13846.
30.   Y. Gu, Y. Katsura, T. Yoshino, H. Takagi and K. Taniguchi, *Sci. Rep.*, 2015, **5**, 12486.
31.   D. Gonbeau, C. Guimon, G. Pfister-Guillouzo, A. Levasseur, G. Meunier and R. Dormoy, *Surf. Sci.*, 1991, **254**, 81.
32.   E. Agostinelli, C. Battistoni, D. Fiorani, G. Mattogno and M. Nogues, *J. Phys. Chem. Solids*, 1989, **50**, 269.
33.   H. Iwakuro, C. Tatsuyama and S. Ichimura, *Jpn. J. Appl. Phys.*, 1982, **21**, 94.
34.   T. Björkman, A. Gulans, A. V. Krasheninnikov and R. M. Nieminen, *Phys. Rev. Lett.*, 2012, **108**, 235502.
35.   R. Brec, G. Ouvrard, J. Ritsma and J. Rouxel, *Rev. Chim. Miner.*, 1976, **13**, 348.
36.   X. Huang, Z. Zeng and H. Zhang, *Chem. Soc. Rev.*, 2013, **42**, 1934.
37.   Z. Zeng, Z. Yin, X. Huang, H. Li, Q. He, G. Lu, F. Boey and H. Zhang, *Angewandte Chemie International Edition*, 2011, **50**, 11093.
38.   J. Wang, J. Polleux, J. Lim and B. Dunn, *J. Phys. Chem. C*, 2007, **111**, 14925.
39.   S. Das, S. Majumder and R. Katiyar, *J. Power Sources*, 2005, **139**, 261.
40.   R. Sun, Q. Wei, J. Sheng, C. Shi, Q. An, S. Liu and L. Mai, *Nano Energy*, 2017, **35**, 396.

Entry for the Table of Contents (Please choose one layout)

Layout 1:

FULL PAPER

The sodium storage capability of TiSe$_2$ is studied for the first time. The combined in-situ XRD and ex-situ HRTEM results suggest that sodium storage is achieved through a multi-step intercalation/deintercalation mechanism. Besides, bulk TiSe$_2$ is easily exfoliated into nanosheets, and might be a promising 2D material platform for energy and electronic applications.
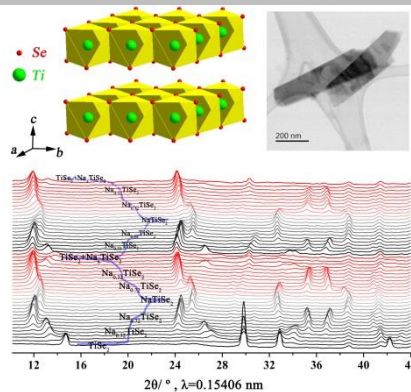
Dan Zhang,[+] Guoqiang Zhao,[+] Peng Li, Yu Zhang, Wenbin Qiu, Jie Shu, Yinzhu Jiang,* Shi Xue Dou, Wenping Sun*

Page No. – Page No.

Readily Exfoliated TiSe$_2$ Nanosheets for High-Performance Sodium Storage